ACADEMIC PRESS

Available online at www.sciencedirect.com

SCIENCE DIRECT®

VIROLOGY

Virology 306 (2003) 334–346

www.elsevier.com/locate/yviro

Comparative histopathological studies in the early stages of acute pathogenic and nonpathogenic SHIV-infected lymphoid organs

Toshihide Shimada,[a] Hajime Suzuki,[b] Makiko Motohara,[b] Takeo Kuwata,[b] Kentaro Ibuki,[b] Masahiro Ui,[b] Tohko Iida,[c] Manabu Fukumoto,[d,1] Tomoyuki Miura,[b,*] and Masanori Hayami[b]

[a] *Department of Pathology, Kyoto City Hospital, Kyoto 604-8845, Japan*
[b] *Institute for Virus Research, Kyoto University, Sakyo-ku Kyoto 606-8507, Japan*
[c] *Department of Microbiology, Kyoto Prefectural University of Medicine, Kyoto 602-8566, Japan*
[d] *Department of Pathology and Biology of Diseases, Graduate School of Medicine, Kyoto University, Kyoto 606-8507, Japan*

Received 8 February 2002; returned to author for revision 1 July 2002; accepted 18 July 2002

Abstract

To clarify the early pathological events in simian and human immunodeficiency chimeric virus (SHIV)-infected lymphoid organs, we examined rhesus macaques infected with an acute pathogenic SHIV (SHIV89.6P) or a nonpathogenic SHIV (NM-3rN) by sequential biopsies and serial necropsies. In the SHIV89.6P-infected monkeys, acute thymic involution as shown by increased cortical tingible-body macrophages and by neutrophilic infiltrates without follicular aggregation in the medulla began within 14 days postinoculation (dpi). Cells that were strongly positive for the virus were identified in the thymic medulla. SHIV89.6P-infected lymph nodes showed severe paracortical lymphadenitis with scattered virus-positive cells at 14 dpi and they developed paracortical depletion without the obvious follicular involution. In contrast, NM-3rN-infected monkeys showed no signs of thymic dysinvolution and the lymph nodes exhibited only follicular hyperplasia. NM-3rN-infected monkeys showed much fewer virus-positive cells in these lymphoid tissues than did SHIV89.6P-infected monkeys during the same period. These differences clearly reflect the difference in the virulence of these SHIVs.

Keywords: AIDS; HIV; SIV; Animal model; Rhesus monkey; Pathology

Introduction

Investigations of the early events in human immunodeficiency virus (HIV) infection can provide important clues to understanding the resultant disease progression and prognosis (Fauci, 1993; Graziosi et al., 1998; Pantaleo et al., 1993). However, detailed studies of HIV-infected humans at the early stage are extremely limited and even impossible to conduct during the first few weeks (Madea et al., 1990; Prevot et al., 1992). Simian immunodeficiency viruses (SIVs) are closely related to HIVs and some of them are known to cause a fatal disease in infected macaques similar to those seen in human acquired immunodeficiency syndrome (AIDS) (Daniel et al., 1985; Letvin et al., 1985; Letvin and King, 1990; Ringler et al., 1989; Wyand et al., 1989). Extensive studies on the early infection course have been done in macaques to help understand the early infection course in humans (Chakrabarti et al., 1994; Lackner et al., 1994). However, the immune response of monkeys to SIV envelope proteins is thought to be different from the immune response of humans to HIV-1 (Weiss et al., 1986). Thus, for developing anti-HIV-1 drugs and vaccines and for evaluating their efficacy and safety, a new animal model that utilizes the HIV-1 genes would be valuable.

To establish an experimental vaccination model using HIV-1 and macaque monkeys, we have developed a series of SIVmac/HIV-1 chimeric viruses (SHIVs) (Haga et al., 1998; Igarashi et al., 1996, 1994; Sakuragi et al., 1992; Shibata et al., 1991). One of these viruses, NM-3rN, carries

* Corresponding author. Fax: +81-75-761-9335.
E-mail address: tmiura@virus.kyoto-u.ac.jp (T. Miura).
[1] Present address: Department of Pathology, Division of Pathophysiology, Institute of Development, Aging and Cancer, Tohoku University.

0042-6822/03/$ – see front matter © 2003 Elsevier Science (USA). All rights reserved.
doi:10.1016/S0042-6822(02)00082-X

the region of intact HIV-1 (NL432) that contains *vpr, tat, rev, vpu,* and *env* (Kuwata et al., 1995). In human and macaque peripheral blood mononuclear cells (PBMCs) as well as in some human T-cell lines, NM-3rN replicated effectively. Its replication was comparable to that of SIVmac239 in vitro. NM-3rN-infected monkeys exhibited viremia and the virus was consistently reisolated from these monkeys during the first several weeks postinfection. Nevertheless, none of the infected monkeys showed significant CD4+ T cell depletion or developed AIDS during more than three years of observation (Haga et al., 1998; Hayami et al., 1999). Taken together, these results indicated that NM-3rN should be classified as a persistently infecting but nonpathogenic SHIV.

In addition to being used to develop HIV vaccine candidates, SHIVs have also been used in vivo to explore the pathogenicity of HIV-1 (Harouse et al., 2001; Igarashi et al., 1999; Joag et al., 1996; Reimann et al., 1996a). Reimann et al. succeeded in developing the first pathogenic SHIV (SHIV89.6P) by serial in vivo passages of the original SHIV-89.6 strain (Reimann et al., 1996b). In contrast to NM-3rN, SHIV89.6P replicated much less than SIVmac239 in macaque PBMCs but replicated well in vivo. The virus caused a rapid and profound CD4+ decline within a couple of weeks and then caused miscellaneous opportunistic infections. Thus, SHIV89.6P was considered an acute pathogenic virus. In a postmortem histopathological examination 169 days postinoculation (dpi), Reimann et al. (1996a, b) observed severe thymic dysinvolution and marked histiocytic paracortical expansion in the infected lymph nodes (LNs). However, the mode of disease progression in the early phase of infection was not clear.

The objective of this study was to clarify the early pathological events in both acute pathogenic and nonpathogenic SHIV-infected lymphoid tissues. We inoculated young rhesus macaques with the acute pathogenic SHIV89.6P or the nonpathogenic NM-3rN and compared the results with those obtained from monkeys infected with a chronic pathogenic molecular clone, SIVmac239. We examined the animals by sequential biopsies and by serial necropsies to explore the histopathology and virus distribution in the lymphoid organs. We observed distinct pathological findings and distinct virus-positive cell populations that reflect the marked difference of their virulence.

Results

Peripheral CD4+ cell count and plasma virus load of infected animals

In all four SHIV89.6P-infected monkeys, peripheral blood CD4+ T cells were depleted within 2 weeks (Fig. 1). Two out of three SIVmac239-infected animals showed a transient CD4+ T cell decline while NM-3rN-infected macaques did not show any significant change of CD4+ T cell counts. As the CD4+ cells were declining in the SHIV89.6P-infected monkeys, the viruses were actively replicating. By the end of the second week, the viruses reached their peak levels, more than 10^9 viral RNA copies per milliliter. In contrast, the peak virus load in the NM-3rN-infected monkeys was delayed and less than 10^7 copies/ml, while the peak titer of SIVmac239-infected monkeys showed intermediate properties (the peak titer of the SIVmac239-infected monkeys at 7 dpi was lower than the peak titer of SHIV89.6P-infected monkeys at 14 dpi but higher than that of NM-3rN-infected monkeys at 18 or 23 dpi). Acute infections with the inoculated viruses were also confirmed by virus reisolation at 14 and 21 dpi in all of these animals.

Histopathological changes of the infected thymus

Both of the SHIV89.6P-infected monkeys that developed AIDS (MM130 and MM131) had severe thymic involution (Table 1). Figure 2A shows representative thymic alterations at the AIDS stage caused by SHIV89.6P infection. The thymic parenchyma showed complete obsolescence and was replaced by aggregations of foamy histiocytes. Although the thymuses of the two SIVmac239-infected animals (MM082 and MM105) showed moderate thymic involution (Table 1 and Fig. 2B, left), they showed severe pneumonia and *Pneumocystis carinii* pneumonia around 630 dpi and were judged as having AIDS (Fig. 2B, right). In contrast to these pathogenic viruses, NM-3rN-infected monkeys did not show any symptoms associated with AIDS during an observation period of more than 3 years (Table 1). To understand how the virus-infected organs changed during the early stage of infection, the SHIV89.6P-infected thymuses were examined at 14 and 28 dpi. In both monkeys necropsied at 14 dpi, we observed acute thymic involution with a “starry sky” appearance in the cortex (Table 2, Fig. 3A, left and middle). The so-called starry sky appearance was due to the abundance of tingible-body macrophages in the cortex. This was consistent with our observation of a significant increase of apoptotic cells in the infected cortex at 14 dpi (Iida et al., 2000). Expansion of the medulla was observed with infiltrations of neutrophilic inflammatory cells that were associated with the nuclear debris of dead cells (Fig. 3A, right). Subsequently, the continuous progression of thymic involution resulted in severe atrophy at 28 dpi (Table 2 and Fig. 3C, left). Thus, acute thymic involution began within 14 dpi and resulted in an accelerated thymic atrophy. In contrast to the SHIV89.6P-infected animals, neither the NM-3rN-infected animals nor the SIVmac239-infected animals developed thymic alterations to such an extent within the observation periods (Table 2, Fig. 3C, middle and right). These findings in the SIVmac239-infected thymuses were consistent with the findings of a previous report (Lackner et al., 1994).

The tissue distribution of the virus-producing cells (VPCs) in the infected thymuses was analyzed by histo-

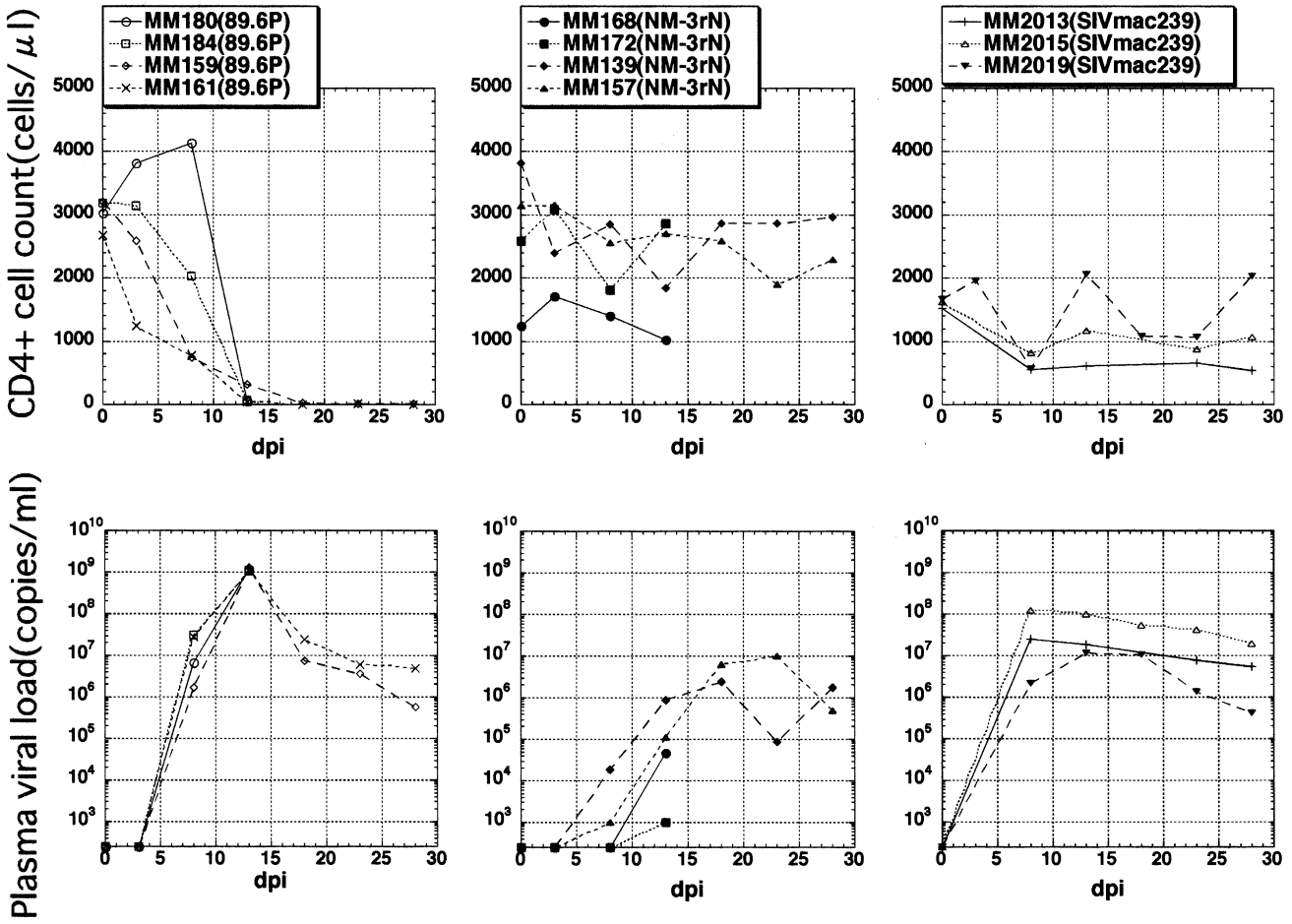

Fig. 1. Kinetics of the peripheral CD4+ cell counts and plasma virus loads in each of the virus-infected monkeys. These parameters were monitored during the observation period of each monkey up to the day of sacrifice.

chemical in situ hybridization (HISH). As shown in Figs. 3B and 3C, in the SHIV89.6P-infected monkeys, the VPCs were localized mainly in the thymic medulla at 14 and 28 dpi. At 14 dpi, the VPCs showed a spindle morphology and were arranged in a network pattern adjacent to Hassall's corpuscles, while much fewer VPCs were observed in the cortex (Fig. 3B). At 28 dpi, the VPCs were scattered in the thymic medulla (Fig. 3C left). The appearance of these VPCs was also associated with the cystic degeneration of the Hassall's corpuscles. In contrast to the pathogenic virus-infected thymuses, the NM-3rN-infected thymuses had only a few VPCs per section (Fig. 3C, middle). In the SIVmac239-infected animals, no obvious histological alteration was observed but scattered VPCs with a small round morphology were identified mainly in the medulla (Fig. 3C, right).

Thymic epithelial cells of the SHIV89.6P-infected monkey, as observed with transparent electron microscopy (TEM), were morphologically classified according to a previous description (Shimosato and Mukai, 1997) (Fig. 4).

Table 1
Disease states of SHIV- and SIV-infected monkeys that were observed for periods of 6 months or more

Animal ID	Inoculated virus	Observation period	Disease state
MM130	SHIV/89.6P, 10 $TCID_{50}$ IV[a]	182 days	AIDS
MM131	SHIV/89.6P, 10 $TCID_{50}$ IV	287 days	AIDS
MM043	SHIV/NM-3rN, 10^5 $TCID_{50}$ IV	1239 days	AC[b]
MM064	SHIV/NM-3rN, 10^5 $TCID_{50}$ IV	1239 days	AC
MM082	SIVmac239, 10^5 $TCID_{50}$ IV	630 days	AIDS
MM105	SIVmac239, 10^5 $TCID_{50}$ IV	630 days	AIDS

[a] IV, intravenous inoculation.
[b] AC, asymptomatic carrier.

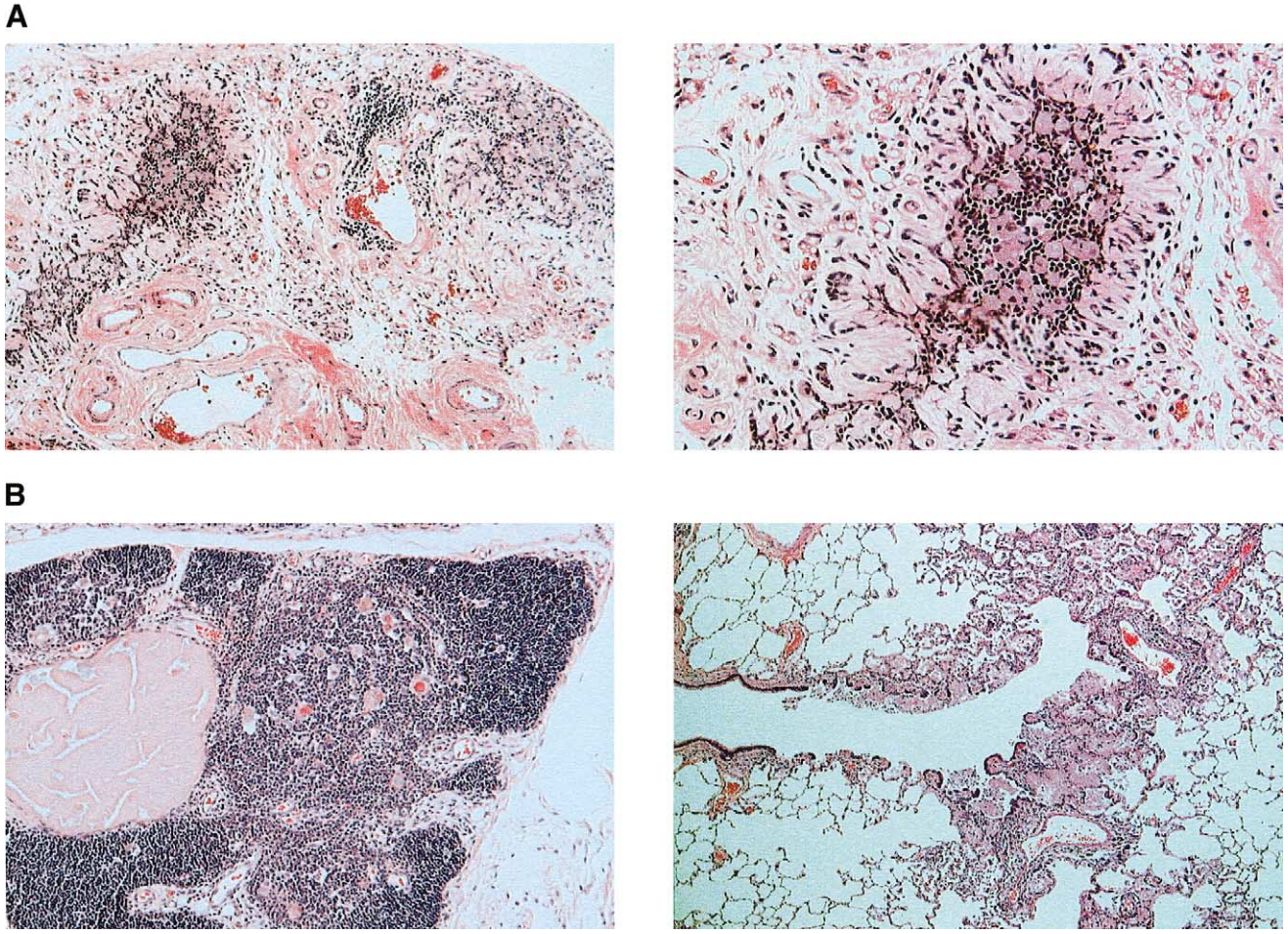

Fig. 2. (A) Involuted thymus in the SHIV89.6P-infected monkey after developing AIDS (MM131). Hematoxylin- and eosin staining (H&E): left, ×40; right, ×400. (B) The involuted but not completely obsolescent thymus derived from a SIVmac239-infected monkey that developed AIDS (MM105; left, ×40). Right panel shows the lung of the same monkey. The terminal airways were filled by *Pneumocystis carinii* (H&E, ×40).

The dark epithelial cells (E4) adjacent to Hassall's corpuscles (H) and the large medullary epithelial cells (E6) seemed to be well preserved at 14 dpi (Fig. 4, left). At 28 dpi, the E4 cells were shrunken and the network structure was distorted (Fig. 4, upper right). In contrast, the subcapsular E1 and pale E2 cell network in the outer cortex seemed to be rather preserved (Fig. 4, lower right). Thus, the disappearance of the VPCs seemed to be in proportion to the disorganization of the thymic medullary epithelial cells.

Histopathological changes of the infected lymph nodes (LNs)

In the SHIV89.6P-infected LNs, remarkable morphologic change was evident from 14 dpi (Table 3 and Fig. 5, upper left). At 14 dpi, the infected nodes revealed a relative paracortical expansion with infiltration of mixed cell types, and there was a severe cell loss at 28 dpi (Fig. 5, lower left). Unlike the HIV- and/or SIV-infected LNs, there was no association of the florid follicular expansion followed by severe involution and depletion. In contrast to the profound CD4+ T cell decline in the peripheral blood within 14 dpi, the cell density in the LNs was rather constant. On the other hand, the NM-3rN-infected LNs showed gradual paracortical expansion at 14 and 28 dpi (Table 3 and Fig. 5, middle). The histology was consistent with chronic nonspecific lymphadenitis and seemed to show mild lymphoid activation. Nevertheless, within this observation period, none of the NM-3rN-infected LNs developed paracortical depletion as the pathogenic SHIV89.6P-infected animals did. The SIVmac239-infected animals exhibited paracortical expansion and sinus histiocytosis at 28 dpi and did not develop the florid follicular hyperplasia that was seen in the persistent generalized lymphadenopathy (PGL) state (Table 3 and Fig. 5, right).

Most of the LNs examined by HISH showed VPCs. The VPCs were mainly in the paracortex, but the ways in which the distributions changed with time differed among the viruses. As previously reported (Chakrabarti et al., 1994; Lackner et al., 1994), in the SIVmac239-infected animals, most of the VPCs were identified in the paracortex at 28 dpi (Table 3 and Fig. 5, lower right). This was more frequent

Table 2
Histopathology and distribution of virus-producing cells in infected lymphoid organs

Virus	Animal ID	dpi	Thymus		Spleen		Tonsil	
			Histopath C/M	HISH C/M	Histopath FL/PALS/RP	HISH FL/PALS/RP	Histopath FL/IF	HISH FL/IF
SHIV89.6P	MM180	14	TBM/IN	+/+++	NP/HM/NP	−/+/−	NA	NA
	MM184	14	TBM/IN	NA	H/HM/NP	−/−/−	H/HM	−/−
	MM159	28	MA/SA	+/++	DP/DP/NP	−/+/−	DP/DP	−/±
	MM161	28	MA/SA	+/++	DP/DP/NP	−/−/−	NA	NA
NM-3rN	MM168	14	NP/NP	−/−	NP/HM/NP	−/−/−	H/HM	−/−
	MM172	14	NP/NP	−/−	H/HM/IN	−/±/−	H/HM	−/±
	MM139	28	NP/NP	−/−	H/NP/NP	±/±/−	H/HM	±/±
	MM157	28	NP/NP	−/−	NP/NP/NP	−/−/−	H/HM	−/−
SIVmac239	MM2013	28	NA	NA	NP/NP/IN	−/±/−	H/HM	+/++
	MM2015	28	NP/NP	−/+	NP/HM/IN	−/+/−	NP/HM	+/++
	MM2019	28	NA	NA	H/HM/IN	−/+/−	H/HM	+/+++

Note. Abbreviations for anatomical sites: C, cortex; M, medulla; FL, follicles; PALS, periarteriolar lymphoid sheath; RP, red pulp; IF, interfollicular area. Histopath, histopathological grading for lymphoid morphology. The histopathological findings for each component are indicated as follows: NP, normal appearance; TBM, tingible body macrophages; IN, infiltration of the neutrophils; MA, moderate atrophy; SA, severe atrophy with lobular collapse; HM, hyperplasia with mixed cell infiltration; H, hyperplasia; DP, depletion; NA, samples not available for study. HISH, histochemical in situ hybridization. Results of HISH were quantified as follows: (−) no positive cell; (±) 1 to 5 positive cells per section; (+) 1 to 5 positive cells per high-power field (HPF = ×400 magnification); (++) 6 to 15 positive cells per HPF; (+++) greater than 15 positive cells per HPF.

than that observed in thymic medulla (Fig. 3C, right). This finding was also consistent with the findings of previous reports (Karr et al., 1994). In the SHIV89.6P-infected LNs, the VPCs transiently increased in number and intensity at 14 dpi and then decreased at 28 dpi. This seemed to be caused by a massive cell loss in the paracortex (Table 3 and Fig. 5, left). On the other hand, in the NM-3rN-infected LN, very few VPCs were detected in the paracortex at 14 and 28 dpi (Fig. 5, middle).

Histopathological changes of the infected spleen and tonsils

It is thought that one of the functions of the spleen is to protect individuals from blood-borne pathogens. The splenocytes are also the target in humans infected with HIV and in monkeys infected with SIV. As reported previously, in the SIVmac239-infected spleen, the VPCs were mainly identified in the periarteriolar lymphoid sheath (PALS), which is a T-cell-dependent zone (Table 2). The SHIV89.6P-infected spleens also exhibited a severe cell loss of PALS at 28 dpi, apparently in parallel with the paracortical depletions in the peripheral LNs. Half of the SHIV89.6P-infected animals showed VPCs in the PALS. In contrast, the NM-3rN-infected spleens exhibited few VPCs distributed in the PALS and showed nonspecific lymphoid activation but never exhibited severe cell loss during the observation periods.

It has been reported that HIV-1-induced changes were more accelerated in the tonsils than in the peripheral LN (Wenig et al., 1996). In three SIVmac239-infected monkeys that were tested in this study, the numbers of VPCs in the tonsils were almost the same as the numbers seen in the corresponding peripheral LNs (Tables 2 and 3). In the SHIV89.6P-infected tonsils, there was clear depletion of mononuclear cells in the paracortex by 28 dpi while only a few VPCs were identified in the same area. On the other hand, in the NM-3rN-infected tonsils, lymphoid activation was the main feature and the frequency of the VPCs was as low as it was in other lymphoid tissues. These findings seem to be similar to what was observed in the paracortex of the peripheral LNs.

Amount of proviral DNA in lymphoid tissues

The amounts of proviral DNA in some lymphoid tissues of infected monkeys were examined by TaqMan PCR (Fig. 6). As expected, the amounts of proviral DNA of all tissues examined were much higher in SHIV89.6P-infected monkeys than in NM-3rN-infected monkeys at all stages. The amounts of proviral DNA in NM-3rN-infected lymphoid tissues were kept at quite low levels during the observation period. In both virus-infected monkeys, the amount of provirus tended to be higher in the thymus than in the spleen and mesenteric LNs at the acute phase of infection, while it tended to be higher in mesenteric LNs at the late stage.

Discussion

The early stage of SHIV89.6P infection was clinically characterized by rapid, profound, and continuous peripheral CD4+ T cell depletion. Reimann et al. (1996a) observed severe thymic dysinvolution (marked atrophy and thymocyte depletion according to their designation) in SHIV89.6P-infected monkeys after 169 dpi. We also noted thymic atrophy and severe paracortical depletion of the peripheral lymph nodes in animals that had developed AIDS. However, the mode of disease

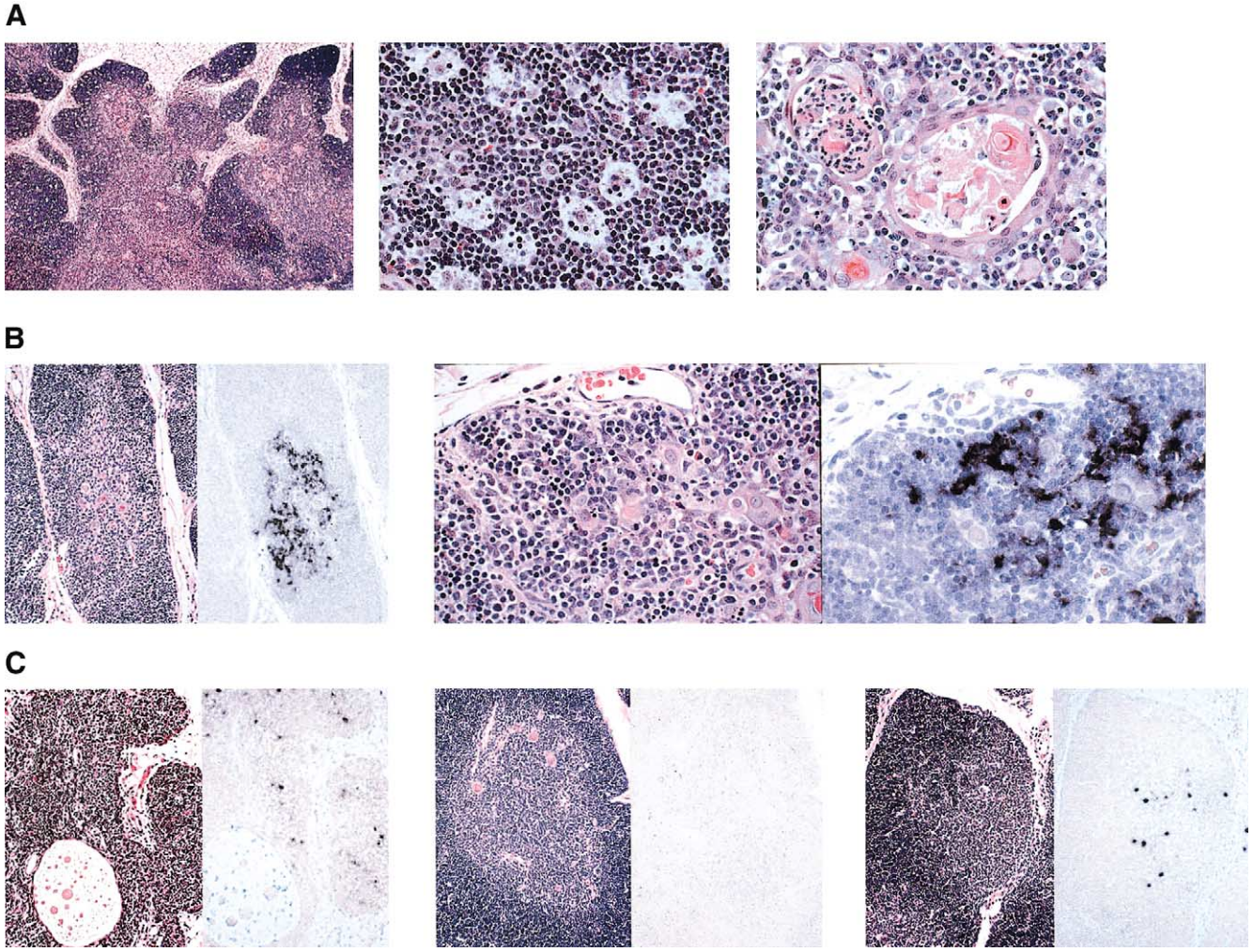

Fig. 3. (A) Representative histology of the early stage of SHIV89.6P-infected thymuses at 14 dpi (H&E). (Left) ×40; (middle) cortex region, ×400; (right) medulla region, ×400. (B, C) Intrathymic distribution of VPCs in the early stage of infection. H&E on left side and histochemical in situ hybridization (HISH) staining on right side are shown, respectively. (B) SHIV89.6P-infected thymus at 14 dpi (left, ×100; right, ×400). (C) SHIV89.6P-infected (left), NM-3rN-infected (middle), and SIVmac239-infected (right) thymus at 28 dpi (×100).

progression was not clear, especially in the early phase of infection. Notably, even the SIV-infected animals that had developed AIDS did not show as much thymic atrophy as was observed in the SHIV89.6P infected animals. In this study, we examined the early stage of pathogenic and nonpathogenic SHIV infections.

All four SHIV89.6P-infected monkeys exhibited severe CD4+ T-cell loss in PBMCs within 14 dpi. Interestingly, despite this observation, the histology of LNs showed paracortical expansion with infiltration of mixed cell types, and the paracortical depletion was delayed to 28 dpi. The peak incidence of the VPCs identified by the HISH analyses seemed to be lower than that seen in the SIVmac239-infected LNs. In fact, most of them disappeared by 28 dpi. Their disappearance was proportional to the paracortical depletion. The paracortical depletion was not found to be associated with either the florid follicular hyperplasia or the resultant follicular depletion, although this type of lesion was usually seen in the SIVmac239 infections. These findings suggest that the profound CD4+ cell depletion in the peripheral blood is a direct reflection of the cell loss caused by the SHIV89.6P infection rather than by redistribution of the infected cells. Wallace et al. (1999) reported that CD4+ T cells are highly activated during acute infection with SHIV89.6PD (a separate isolate of SHIV89.6P) and are unusually susceptible to activation-induced cell death. We previously observed an increased frequency of apoptotic cells in the SHIV89.6P-infected LNs and thymic cortex at the early stage of the infection (Iida et al., 2000). Together, the severe paracortical cell loss without follicular activation seemed to be caused by apoptotic cell death. The high frequency of apoptotic cell death could not be explained only by the cell death directly due to infection with SHIV89.6P because of the low incidence of VPCs.

Our observations indicated that acute thymic involution with a “starry sky” appearance in the cortex prior to severe atrophy was one of the most characteristic in the early stage of SHIV89.6P infection. Thymic involvement has been re-

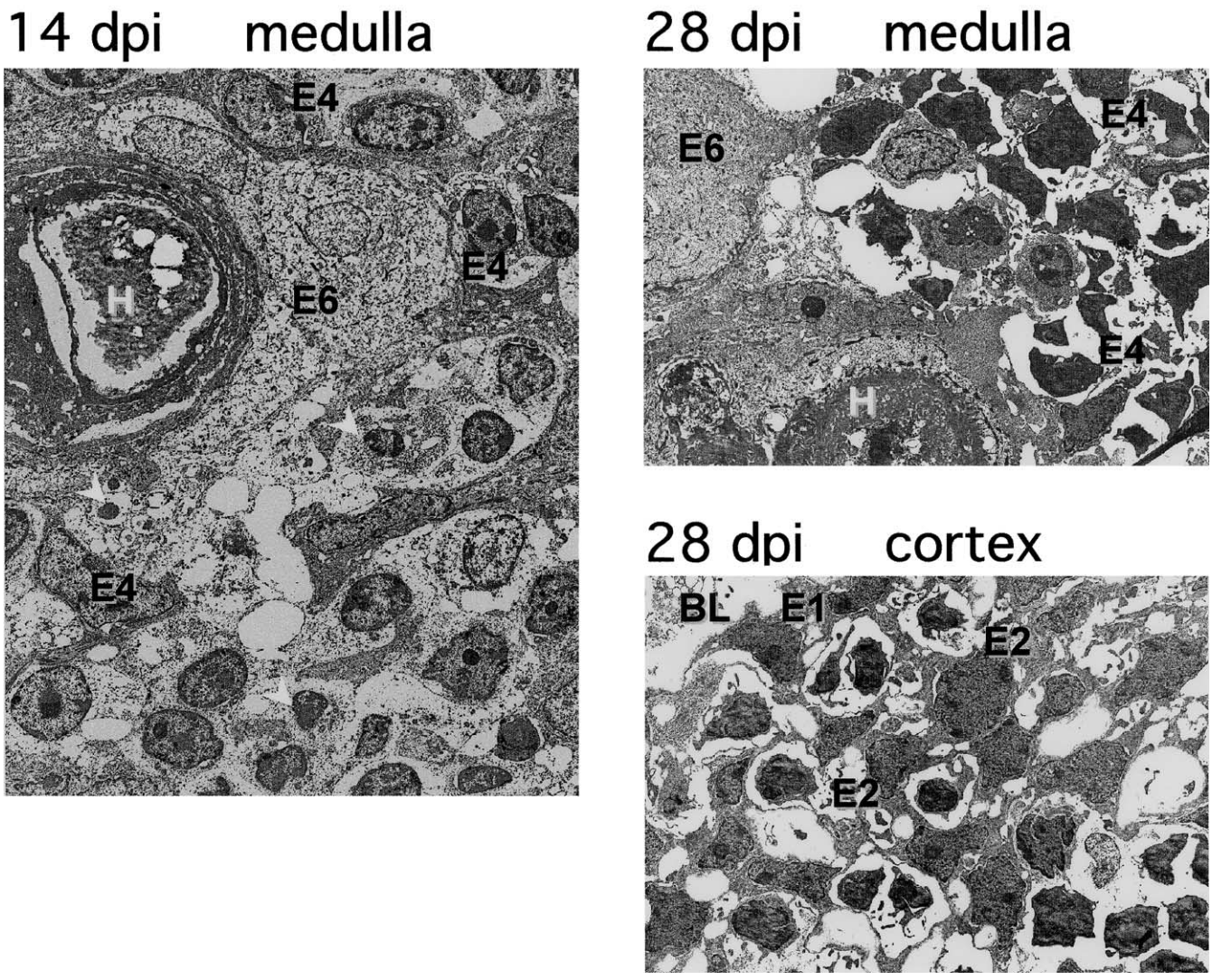

Fig. 4. Representative TEM images derived from SHIV89.6P-infected thymuses at 14 dpi (left) and 28 dpi (right) (×1600). E1, subcapsular cells; E2, pale cells; E4, dark epithelial cells; E6, large medullary epithelial cells; H, Hassall's corpuscles; and BL, basal lamina. The morphological classification of the thymic epithelial cells was according to the reference Shimosato and Mukai (1997).

ported in humans (Burke et al., 1995; Prevot et al., 1992), in macaques (Li et al., 1995; Muller et al., 1993; Wykrzykowska et al., 1998), and in HIV-1-infected thymic implants in SCID-hu mice (Bonyhadi et al., 1993; Ogura et al., 1996). The three major features of the thymic alterations in HIV-infected children and infants are thymitis, precocious thymic involution, and thymic dysinvolution (Joshi et al., 1986). The thymitis was attributed to the formation of lymphoid follicles in the infected medullae. This was observed at a relatively late stage of SIVsm-infected cynomolgous monkeys and seropositive asymptomatic drug addicts (53 to 783 dpi, respectively) (Li et al., 1995; Prevot et al., 1992). One of these studies (Wykrzykowska et al., 1998) described scattered VPCs exhibiting a lymphoid morphology in the medulla as early as 7 dpi. The SHIV89.6P-infected thymuses at this stage did not show a significant follicular aggregation in the medullae as was observed in the SIV-infected animals. Instead, the thymus revealed an abundance of tingible-body macrophages in the cortex accompanied by various degrees of neutrophilic infiltration in the medulla at 14 dpi. This alteration was followed by thymic involution with reduction of VPCs at 28 dpi. Interestingly, the VPCs that were identified in the infected medulla had a spindle shape and a network distribution. Morphologically these seemed to be thymic stromal cells. Similar cell populations and a similar tissue distribution were described in HIV-1-infected thymic implants in SCID-hu mice (Bonyhadi et al., 1993; Okamoto et al., 1998). We noted the peripheral lymphoid depletion in the LNs, spleens, and tonsils in the early stage of SHIV89.6P infections. Taken together, these results seem to indicate that the acute phase of SHIV89.6P infection is characterized by acute thymic involution with generalized lymphoid depletion. In humans, an acute "stress" involution was noted in children undergo-

Table 3
Histopathology and distribution of virus producing cells in sequentially resected peripheral lymph nodes

Virus	Animal ID	Pre-inoculation		5 dpi		14 dpi		28 dpi	
		Histopath FL/PC/S	HISH FL/PC/S	Histopath FL/PC/S	HISH FL/PC/S	Histopath FL/PC/S	HISH FL/PC/S	Histopath FL/PC/S	HISH FL/PC/S
SHIV89.6P	MM180	NP/NP/NP	−/−/−	NP/NP/NP	−/−/−	NP/HM/SH	−/+/−	NA	NA
	MM184	NP/NP/NP	−/−/−	NP/NP/NP	−/−/−	NP/HM/SH	−/+/−	NA	NA
	MM159	NP/NP/NP	−/−/−	NP/NP/NP	−/−/−	NP/HM/SH	−/+/−	H/DP/SH	−/−/−
	MM161	NP/NP/NP	−/−/−	NP/NP/NP	−/−/−	NP/HM/SH	−/+/−	H/DP/SH	−/−/−
NM-3rN	MM168	NP/NP/NP	−/−/−	NP/NP/NP	−/−/−	NP/NP/NP	−/−/−	NA	NA
	MM172	NP/NP/NP	−/−/−	NP/NP/NP	−/±/−	NP/NP/NP	−/−/−	NA	NA
	MM139	NP/NP/NP	−/−/−	NP/NP/NP	−/−/−	NP/NP/NP	−/−/−	NP/H/SH	−/+/−
	MM157	NP/NP/NP	−/−/−	NP/NP/NP	−/−/−	NP/NP/NP	−/−/−	NP/H/SH	−/−/−
SIVmac239	MM2013	NP/NP/NP	−/−/−	NP/NP/NP	−/−/−	NP/H/SH	−/+/−	NP/HM/SH	+/+++/−
	MM2015	NP/NP/NP	−/−/−	NP/NP/NP	−/−/−	NA	NA	NP/HM/SH	+/++/−
	MM2019	NP/NP/NP	−/−/−	NP/NP/NP	−/±/−	NP/H/SH	−/+/−	NP/HM/SH	−/±/−

Note. Abbreviations for anatomical sites: FL, follicles; PC, paracortex; S, sinus. Histopath, histopathological grading for lymphoid morphology. The histopathological findings for each component are indicated as follows: NP, normal appearance; HM, hyperplasia with mixed cell infiltration; SH, sinus histiocytosis; H, hyperplasia; DP, depletion; NA, samples not available for study. The frequencies of VPCs in tissue sections detected by HISH are indicated as described in Table 2.

ing major stress, such as occurs with extensive thermal injury, radiotherapy, anti-tumor therapy, chorioamnionitis, and sepsis (Shimosato and Mukai, 1997; Suster and Rosai, 1992; Toti et al., 2000). The histology of the stress involution was known as acute cortical shrinkage associated with a starry sky appearance, and it was similar to that seen in the SHIV89.6P infection (Fig. 3A and Toti et al., 2000). This accidental or stress-associated involution appears to result from a sudden release of corticosteroid from the adrenal cortex, which causes rapid lympholysis of the cortical thymocytes (Cowan and Sorenson, 1964). Some of the thymic epithelial cells were thought to be secreting thymic peptides, such as thymosin fraction 5, which modulate the hypothalamo–pituitary–adrenal axis by affecting the release of adrenocorticotropic hormone (Goya et al., 1993). Interestingly, we observed densely packed VPCs in the thymic medulla followed by the disruption of the E4 cell network in the SHIV89.6P-infected animals. As mentioned above, the virus did not seem to directly kill many infected cells in the lymph nodes. Taken together, these results suggest that the CD4 depletion in the SHIV89.6P-infected animals is due to stress involution induced by viral infection and that the generation of CD4+ cells in its lineage is inhibited. Expression of interleukin-7, a cytokine produced by thymic stro-

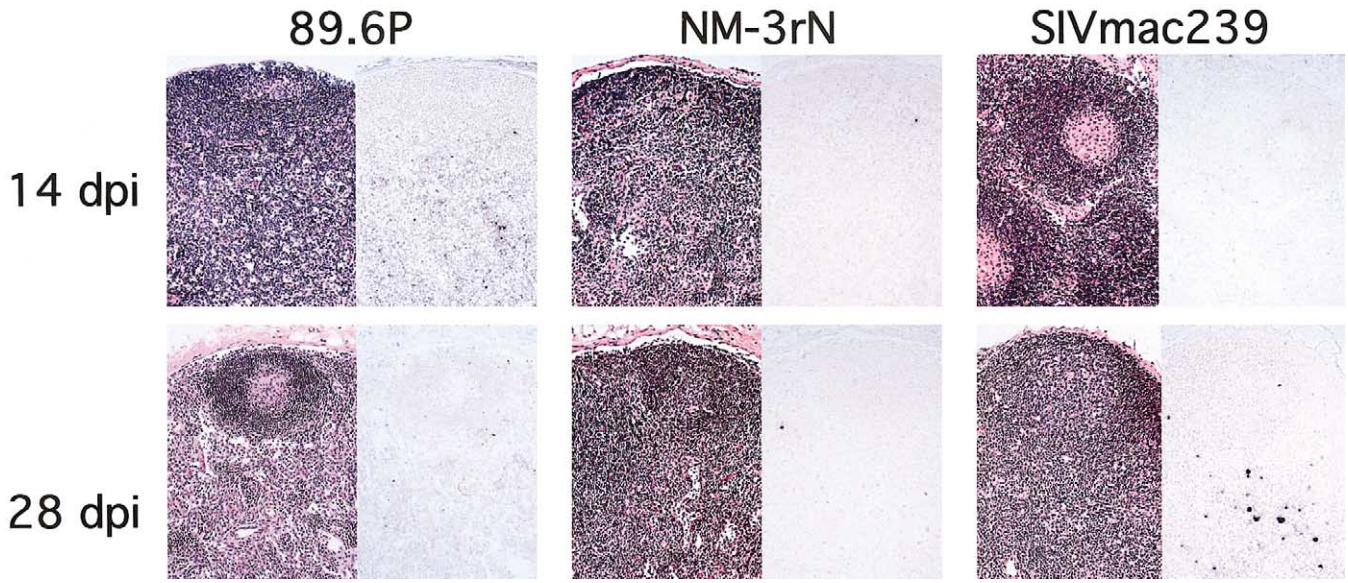

Fig. 5. Representative tissue distributions of VPCs in sequentially resected LNs. The HISH staining of the sequentially resected LNs is shown. SHIV89.6P-, NM-3rN-, and SIVmac239-infected LNs are arranged from left to right, respectively. The left-side image in each panel shows H&E at the indicated period, while the right-side image shows HISH of sequential sections.

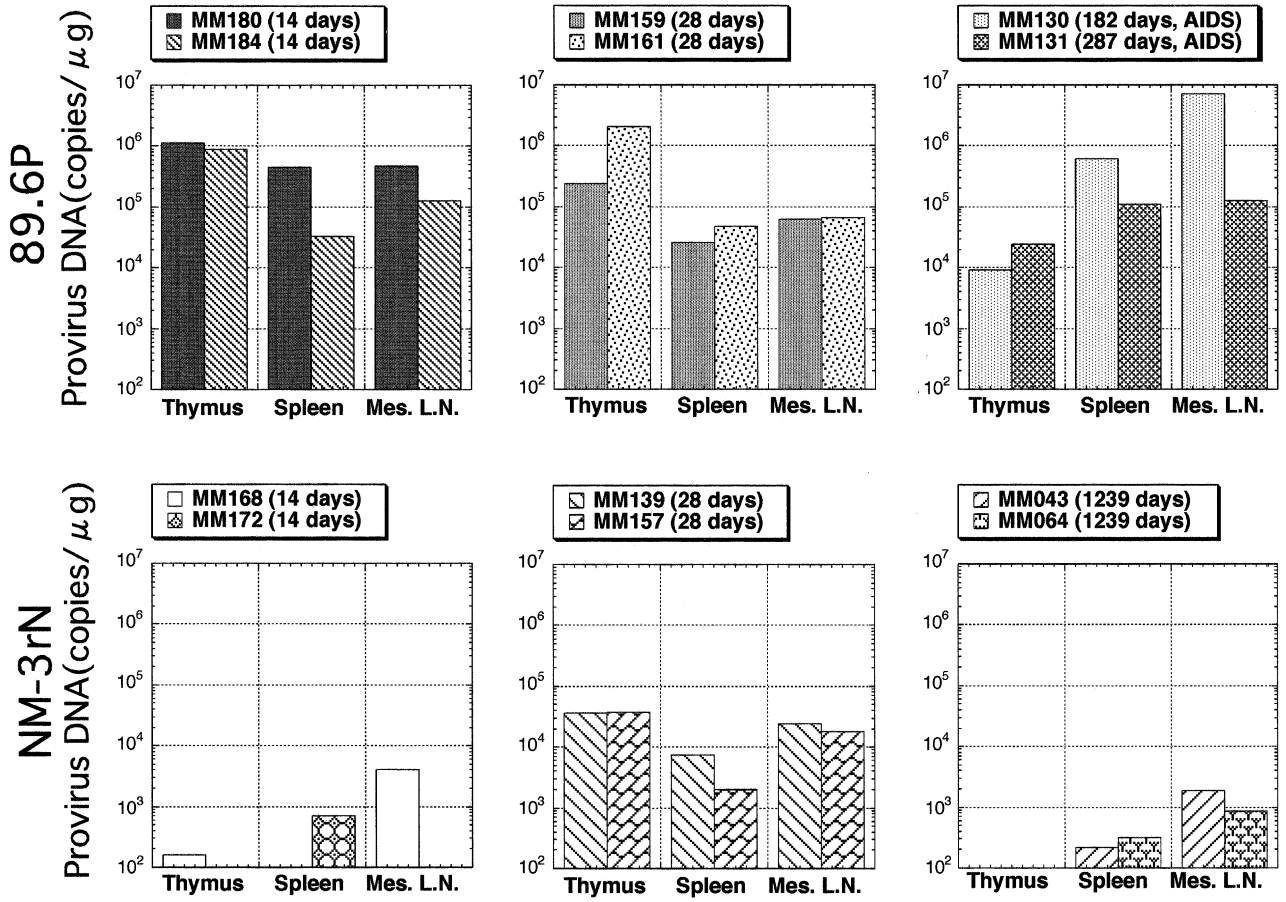

Fig. 6. Proviral DNA quantification in SHIV89.6P- or NM-3rN-infected lymphoid tissues (thymus, spleen, and mesenteric LN).

mal cells and known to play a key role in T cell development, in HIV-1-positive individuals correlates with CD4+ T cell depletion (Llano et al., 2001). Further investigations are needed to clarify the humoral factors involved in immune modulations.

As the thymic atrophy caused by the SHIV89.6P infection was so profound, the regeneration of the T cell pool would be expected to be impaired and the resultant T cell repertoire would be expected to be extremely limited. Such a limitation together with the paracortical depletion of the lymph nodes might explain the rapid, profound, and "continuous" T cell depletion in the SHIV89.6P-infected animals. This rapid and drastic clinical course is clearly different from that observed in HIV-1-infected humans. However, SHIV and HIV-1 share several properties: SHIV has several HIV-1 genes including *env*, the same CD4+ T lymphocyte subset that is depleted in HIV-1-infected humans is depleted in SHIV-infected monkeys, and the symptoms of the induced immunodeficiency in the SHIV-infected monkeys are also very similar to those observed in HIV-1-infected individuals (Douek et al., 1998). Furthermore, the infectivity of thymocytes was found to be closely associated with the CD4 depletion by HIV-1 in vivo (Stoddart et al., 2001). Therefore, the acute pathogenicity of SHIV89.6P in macaques can be viewed as a model of human AIDS with a markedly compressed clinical course and should be quite useful for further investigation of the in vivo mechanism of AIDS pathogenesis.

As we reported previously, NM-3rN replicated as fast as the parental SIVmac239 in human and macaque PBMCs and in several CD4+ human cell lines (Kuwata et al., 1995). Chronic persistent infections have been established in rhesus, pig-tailed, and cynomolgous monkeys (Hayami et al., 1999; Kuwata et al., 1995). In the very early stage of infection, the cell-associated virus loads of NM-3rN were comparable with those of SIVmac239 and they thereafter declined to a 10- to 100-fold lower level (Kuwata et al., 1995), while the plasma virus load, which is more sensitive than the cell-associated virus load, showed that NM-3rN has a lower growth ability in vivo (Fig. 2). Our study indicated that there was an activation of the infected LNs (as demonstrated by paracortical expansion with mixed cellular infiltration) at 28 dpi in both the NM-3rN- and SIVmac239-infected animals. The NM-3rN-infected monkeys subsequently showed follicular hyperplasia in the chronic state of infection. Nevertheless, the infected germinal centers did not show any involuted features and the frequencies of occurrence of VPCs and the amounts of proviral DNA were

significantly lower than those seen in the pathogenic SHIV89.6P-infected monkeys. The generalized lymphoid activation with the minimal involution and reduced frequency of VPCs in the lymphoid tissues seemed to be the main features of the NM-3rN infection. These results were similar to those observed in human long-term nonprogressors (Pantaleo et al., 1995). Thus, the in vivo NM-3rN proliferation did not cause extreme lymphoid activation such as persistent generalized lymphadenopathy, and therefore it may provide a good model for long-term nonprogressors. Further studies are needed to clarify the mode of infection at the early stage of long-term nonprogressive infection, which cannot be predicted in humans.

The tissue distributions of SHIV89.6P and SIVmac239 were clearly different although the viral load set points at 28 dpi for the two viruses were similar. The different tissue tropisms of these viruses seem to be due to a difference in the coreceptors that they use. That is, SIVmac239 uses CCR5, and SHIV89.6P uses both CCR5 and CXCR4. Other acute pathogenic SHIV strains causing rapid CD4+ cell depletion are also known to use CXCR4 only or both CXCR4 and CCR5, whereas infection with a pathogenic CCR5-specific enveloped virus, SHIVSF162P, caused a dramatic loss of CD4+ intestinal T cells followed by a gradual depletion in peripheral CD4+ T cells (Harouse et al., 1999; Igarashi et al., 1999; Joag et al., 1996). NM-3rN has the env of an HIV-1 strain that is derived from the NL432 strain and uses CXCR4 as a coreceptor but replication of NM-3rN in vivo is limited. The rapid CD4+ T cell depletion that occurs in peripheral blood at the early stage of infection may require the usage of the CXCR4 coreceptor and a high virus load set point.

In conclusion, the early stage of the SHIV89.6P infection was characterized by acute thymic involution and paracortical lymphadenitis which began within 14 dpi. Because of the severe pathological alterations and the profound peripheral CD4+ cell loss caused by SHIV89.6P, the infection in macaques is useful for analyzing the in vivo mechanism of AIDS pathogenesis. In contrast, NM-3rN showed generalized lymphoid activation with minimal involution and these pathological findings were similar to those seen in human long-term nonprogressors. NM-3rN induced strong immunological responses and resulted in minimal cell loss caused by apoptosis. Clarification of the mechanisms responsible for the disease-free state in NM-3rN infection might provide insights for preventing pathogenic virus infections. Also, the nonpathogenic features of NM-3rN might make this virus suitable as a prototype for live-attenuated vaccines.

Materials and methods

SHIV

The detailed protocol for generation of NM-3rN has been described (Kuwata et al., 1995). SHIV89.6P was kindly provided by Dr. K.A. Reimann and Dr. N.L. Letvin (Reimann et al., 1996a). The pathogenic molecular clone, SIVmac239, was kindly provided by Dr. R.C. Desrosiers (Naidu et al., 1988). The plasmid DNAs of NM-3rN and SIVmac239 were transfected into M8166 cells (Clapham et al., 1987) and infectious viruses were obtained. Rhesus macaque PBMCs were infected with these viruses and the supernatant with the highest reverse transcriptase activity level was used as the virus stock. The $TCID_{50}$ values of these stock viruses were determined using M8166 cells and were adjusted by adding an appropriate volume of medium.

Animal experiments

Monkeys were treated in accordance with the institutional regulations approved by the Committee for Experimental Use of Nonhuman Primate in the Institute for Virus Research, Kyoto University. As references for the AIDS state, two SHIV89.6P-infected monkeys (MM130 and MM131) and two SIVmac239-infected monkeys (MM082 and MM105) were observed until they showed the initial symptoms of the disease. Two NM-3rN-infected monkeys were followed up for more than 3 years (Table 1). A total of eight young rhesus monkeys (*Macaca mulatta,* 3 to 6 years old) were infected with either SHIV89.6P or NM-3rN. Two monkeys for each incubation period (14 and 28 days) were employed. For positive controls of viral infection, we examined three SIVmac239-infected monkeys for 28 days (Tables 2 and 3). All of these monkeys were confirmed to be free of SIV and simian T-cell leukemia/lymphoma virus type 1 (STLV-1). The animals were intravenously inoculated with 10 $TCID_{50}$ of SHIV89.6P or NM-3rN or with 10^5 $TCID_{50}$ of SIVmac239. The peripheral LNs were sequentially removed to examine the histopathological alterations. The blood samples were periodically monitored by CD4+ cell counts and by determining the plasma virus load as described (Kozyrev et al., 2001). At 14 and 28 dpi, the SHIV89.6P- and NM-3rN-infected animals were euthanized and necropsied for subsequent histopathological examinations. The thymus, spleen, tonsil, and peripheral LN (axillary, inguinal, and mesenteric) derived from an identical animal were either fixed in 4% paraformaldehyde (PFA)–PBS overnight at 4°C, and then embedded in paraffin wax for the histological examinations and histochemical in situ hybridization (HISH) studies, or directly frozen for DNA extraction.

Histopathological examination

The tissue sections were cut at a thickness of 4 μm and stained with hematoxylin–eosin (H&E) for the subsequent histopathological examinations. Histological alterations of the viral-infected macaques were classified according to a previous report (Ringler et al., 1989). To examine alterations in the tissue, some of the PFA-fixed and paraffin-

embedded thymic tissues were excised, deparaffinized, and subjected to transparent electron microscopy (TEM).

Histochemical in situ hybridization (HISH)

Digoxigenin-labeled antisense RNA probes were employed for the HISH detection of the viral genomes (DIG–RNA, Böehringer–Mannheim, Tokyo, Japan) (Bucy et al., 1994; Karr et al., 1994). Briefly, 4-μm-thick paraffin sections were deparaffined and subjected to 0.2 M HCl degeneration followed by Proteinase K (PK; Sigma–Aldrich Japan, Tokyo) digestion and acetylation. The conditions of PK treatment (4 μg/ml in PBS at 37°C for 30 min) were determined by preliminary tests. After postfixation, the sections were prehybridized for 1 h at room temperature and hybridized overnight at 42°C with 5 ng/section of the DIG–RNA probes. Following RNase treatment and extensive washing, the hybrids were incubated with alkaline phosphatase-conjugated antidigoxigenin antibody (Fab fractionated) and the resultant complexes were visualized by NBT/BCIP substrates (Böehringer–Mannheim, Tokyo, Japan) at 4°C for 40 h.

For an RNA probe, we synthesized and tested several candidates such as the *gag*, *pol*, or *nef* regions, which were raised against almost identical sequences among SIVmac239, NM-3rN, and SHIV89.6P. We eventually selected a 562-nucleotide region in *nef* because it gave the strongest and most reproducible signals. Viral distributions were estimated by the number of VPCs per high power ($\times$400) field under the microscope.

Quantitative analysis of provirus DNA

The SHIV proviral DNA quantitative assay was performed with TaqMan DNA PCR (Perkin–Elmer, USA) for the SIV gag region using the primers SIVII-696F (5′-GGAAATTACCCAGTACAACAAATAGG-3′) and SIVII-784R (5′-TCTATCAATTTTACCCAAGGCATTTA-3′). DNA samples were extracted directly from frozen lymphoid tissues with a QIAGEN DNeasy Tissue kit (QIAGEN, Germany) according to the manufacturer's protocol. A labeled probe, SIVII-731T (5′-Fam-TGTCCACCTGCCATTAAGCCCG-Tamra-3′), was used for detection of the PCR product. For each run, a standard curve was generated from a plasmid DNA sample containing the full genome of SHIV NM-3rN, which was quantified with a UV spectrophotometer.

Acknowledgments

We sincerely thank Drs. K.A. Reimann and N.L. Letvin of Beth Israel Hospital, Boston, for kindly providing SHIV89.6P. We thank Keijiro Tamaru, Tsutomu Obata, Yoshinobu Toda, and Makio Fujioka for expert assistance in tissue processing and pathological examinations; Kyoko Yokoyama for technical support of quantitative provirus DNA PCR; James Raymond for professional English editing; and Drs. Tatsuhiko Igarashi, Hiromi Kubagawa, R. Pat Bucy, and Cynthia Derdeyn for their helpful discussions and encouragement. This work was supported by grants-in-aid for AIDS research from the Organization for Drug Relief, R&D Promotion and Product Review, a Grant-in-Aid for Scientific Research from the Ministry of Education and Science, Japan, and a Research Grant on Health Sciences focusing on Drug Innovation from Japan Health Sciences Foundation.

References

Bonyhadi, M., Rabin, L., Salimi, S., Brown, D.A., Kosek, J., McCune, J.M., Kaneshima, H., 1993. HIV induces thymus depletion in vivo. Nature 363, 728–732.

Bucy, R.P., Panoskaltsis-Mortari, A., Huang, G.Q., Li, J., Kerr, L., Ross, M., Russel, J.H., Murphy, K.M., Weaver, C.T., 1994. Heterogeneity of single cell cytokine gene expression in clonal T cell populations. J. Exp. Med. 180, 1251–1262.

Burke, A.P., Anderson, D., Benson, W., Turnicky, R., Mannan, P., Liang, Y.H., Smialek, J., Virmani, R., 1995. Localization of human immunodeficiency virus in thymic tissues from asymptomatic drug addicts. Arch. Pathol. Lab. Med. 119, 36–41.

Chakrabarti, L., Isola, P., Cumont, M.C., Claessens-Maire, M.A., Hurtrel, M., Montagnier, L., Hurtrel, B., 1994. Early stages of simian immunodeficiency virus infection in lymph nodes: evidence for high viral load and successive population of target cells. Am. J. Pathol. 144, 1226–1237.

Clapham, P.R., Weiss, R.A., Dalgleish, A.G., Exley, M., Whitby, D., Hogg, N., 1987. Human immunodeficiency virus infection of monocytic and T-lymphocytic cells: receptor modulation and differentiation induced by phorbol ester. Virology 158, 44–51.

Cowan, W.K., Sorenson, G.D., 1964. Electron microscopic observations of acute thymic involution produced by hydrocortisone. Lab. Invest. 13, 353–370.

Daniel, M.D., Letvin, N.L., King, N.W., Kannagi, M., Sehgal, P.K., Hunt, R.D., Kanki, P.J., Essex, M., Desrosiers, R.C., 1985. Isolation of a T-cell tropic HTLV-III-like retrovirus from macaques. Science 228, 1201–1204.

Douek, D.C., McFarland, R.D., Keiser, P.H., Gage, E.A., Massey, J.M., Haynes, B.F., Polis, M.A., Haase, A.T., Feinberg, M.B., Sullivan, J.L., Jamieson, B.D., Zack, J.A., Picker, L.J., Koup, R.A., 1998. Changes in thymic function with age and during the treatment of HIV infection. Nature 396, 690–695.

Fauci, A.S., 1993. Multifactorial nature of human immunodeficiency virus disease: implications for therapy. Science 262, 1011–1017.

Goya, R.G., Castro, M.G., Hannah, M.J., Sosa, Y.E., Lowry, P.J., 1993. Thymosin peptides stimulate corticotropin release by a calcium-dependent mechanism. Neuroendocrinology 57 (2), 230–235.

Graziosi, C., Soudeyns, H., Rizzardi, G.P., Bart, P.-A., Chapuis, A., Pantaleo, G., 1998. Immunopathogenesis of HIV infection. AIDS Res. Hum. Retroviruses 14, 135–142.

Haga, T., Kuwata, T., Ui, M., Igarashi, T., Miyazaki, Y., Hayami, M., 1998. A new approach to AIDS research and prevention: the use of gene-mutated HIV-1/SIV chimeric viruses for anti-HIV-1 live attenuated vaccines. Microbiol. Immunol. 42, 245–251.

Harouse, J.M., Gettie, A., Eshetu, T., Tan, R.C., Bohm, R., Blanchard, J., Baskin, G., Cheng-Mayer, C., 2001. Mucosal transmission and induction of simian AIDS by CCR5-specific simian/human immunodeficiency virus SHIV(SF162P3). J. Virol. 75 (4), 1990–1995.

Harouse, J.M., Gettie, A., Tan, R.C., Blanchard, J., Cheng-Mayer, C., 1999. Distinct pathogenic sequela in rhesus macaques infected with CCR5 or CXCR4 utilizing SHIVs. Science 284 (5415), 816–819.

Hayami, M., Igarashi, T., Kuwata, T., Ui, M., Haga, T., Ami, Y., Shinohara, K., Honda, M., 1999. Gene-mutated HIV-1/SIV chimeric viruses as AIDS live attenuated vaccines for potential human use. Leukemia 13, S42–S47.

Igarashi, T., Endo, Y., Englund, G., Sadjadpour, R., Matano, T., Buckler, C., Buckler-White, A., Plishka, R., Theodore, T., Shibata, R., Martin, M., 1999. Emergence of a highly pathogenic simian/human immunodeficiency virus in a rhesus macaque treated with anti-CD8 mAb during a primary infection with a nonpathogenic virus. Proc. Natl. Acad. Sci. USA 96 (24), 14049–14054.

Igarashi, T., Kuwata, T., Takehisa, J., Ibuki, K., Shibata, R., Mukai, R., Komatsu, T., Adachi, A., Ido, E., Hayami, M., 1996. Genomic and biological alteration of a human immunodeficiency virus type 1 (HIV-1)-simian immunodeficiency virus strain mac chimera, with HIV-1 env, recovered from a long-term carrier monkey. J. Gen. Virol. 77, 1649–1658.

Igarashi, T., Shibata, R., Hasebe, F., Ami, Y., Shinohara, K., Komatsu, T., Stahl-Henning, G., Petry, H., Hunsmann, G., Miura, T., Hayami, M., 1994. Persistent infection with SIVmac chimeric virus having tat, rev, vpu, env and nef of HIV-1 in macaque monkeys. AIDS Res. Hum. Retroviruses 10, 1021–1029.

Iida, T., Ichimura, H., Shimada, T., Ibuki, K., Ui, M., Tamaru, K., Kuwata, T., Yonehara, S., Imanishi, J., Hayami, M., 2000. Role of apoptosis in both peripheral lymph nodes and thymus in progressive loss of CD4+ cells in SHIV-infected macaques. AIDS Res. Hum. Retroviruses 16 (1), 9–18.

Joag, S.V., Li, Z., Foresman, L., Stephens, E.B., Zhao, L.J., Adany, I., Pinson, D.M., McClure, H.M., Narayan, O., 1996. Chimeric simian/human immunodeficiency virus that causes progressive loss of CD4+ T cells and AIDS in pig-tailed macaques. J. Virol. 70 (5), 3189–3197.

Joshi, V.V., Oleske, J.M., Saad, S., Gadol, C., Connor, E., Bobila, R., Minnefor, A.B., 1986. Thymus biopsy in children with acquired immunodeficiency syndrome. Arch. Pathol. Lab. Med. 110 (9), 837–842.

Karr, L.J., Panoskaltsis-Mortari, A., Li, J., Devore-Carter, D., Weaver, C.T., Bucy, R.P., 1994. In situ hybridization for cytokine mRNA with digoxigenin-labeled riboprobes. Sensitivity of detection and double label applications. J. Immunol. Methods 182, 93–106.

Kozyrev, I.L., Ibuki, K., Shimada, T., Kuwata, T., Takemura, T., Hayami, M., Miura, T., 2001. Characterization of less pathogenic infectious molecular clones derived from acute-pathogenic SHIV-89.6p stock virus. Virology 282 (1), 6–13.

Kuwata, T., Igarashi, T., Ido, E., Jin, M., Mizuno, A., Chen, J., Hayami, M., 1995. Construction of human immunodeficiency virus 1/simian immunodeficiency virus strain mac chimeric viruses having vpr and/or nef of different parental origins and their in vitro and in vivo replication. J. Gen. Virol. 76, 2181–2191.

Lackner, L.A., Vogel, P., Ramos, R.A., Kluge, J.D., Marthas, M., 1994. Early events in tissues during infection with pathogenic (SIVmac239) and nonpathogenic (SIVmac1A11) molecular clones of simian immunodeficiency virus. Am. J. Pathol. 145, 428–439.

Letvin, N.L., Daniel, M.D., Sehgal, P.K., Desrosiers, R.C., Hunt, R.D., Waldron, L.M., MacKey, J.J., Schmidt, D.K., Chalifoux, L.V., King, N.W., 1985. Induction of AIDS-like disease in macaque monkeys with T-cell tropic retrovirus STLV-III. Science 230, 71–73.

Letvin, N.L., King, N.W., 1990. Immunologic and pathologic manifestations of the infection of rhesus monkeys with simian immunodeficiency virus of macaques. J. AIDS 3, 1023–1040.

Li, S.L., Kaaya, E.E., Ordonez, C., Ekman, M., Feichtinger, H., Putkonen, P., Bottiger, D., Biberfeld, G., Biberfeld, P., 1995. Thymic immunopathology and progression of SIVsm infection in cynomolgous monkeys. J. AIDS Hum. Retrovirol. 9, 1–10.

Llano, A., Barretina, J., Gutierrez, A., Blanco, J., Cabrera, C., Clotet, B., Este, J.A., 2001. Interleukin-7 in plasma correlates with CD4 T-cell depletion and may be associated with emergence of syncytium-inducing variants in human immunodeficiency virus type 1-positive individuals. J. Virol. 75 (21), 10319–10325.

Madea, B., Roewert, H.J., Krueger, G.R., Ablashi, D.V., Josephs, S.F., 1990. Search for early lesions following human immunodeficiency virus type 1 infection: a study of six individuals who died a violent death after seroconversion. Arch. Pathol. Lab. Med. 114, 379–382.

Muller, J.G., Kernn, V., Schindler, C., Czub, S., Stahl-Henning, C., Coulibaly, C., Hunsmann, G., Kneitz, C., Kerkau, T., Rethwiln, A., ter-Meulen, V., Muller-Hermelink, H.K., 1993. Alterations of thymus cortical epithelium and interdigitating dendritic cells but no increase of thymocyte cell death in the early course of simian immunodeficiency virus infection. Am. J. Pathol. 143, 699–713.

Naidu, Y.M., Kestler III, H.W., Li, Y., Butler, C.V., Silva, D.P., Schmidt, D.K., Troup, C.D., Sehgal, P.K., Sonigo, P., Daniel, M., Desrosiers, R.C., 1988. Characterization of infectious molecular clones of simian immunodeficiency virus (SIVmac) and human immunodeficiency virus type 2: persistent infection of rhesus monkeys with molecularly cloned SIVmac. J. Virol. 62, 4691–4696.

Ogura, A., Noguchi, Y., Yamamoto, Y., Shibata, S., Asano, T., Okamoto, Y., Honda, M., 1996. Localization of HIV-1 in human thymic implant in SCID-hu mice after intravenous inoculation. Int. J. Exp. Pathol. 77, 201–206.

Okamoto, Y., Eda, Y., Ogura, A., Shibata, S., Amagai, T., Katsura, Y., Asano, T., Kimachi, K., Makizumi, K., Honda, M., 1998. In SCID-hu mice, passive transfer of a humanized antibody prevents infection and atrophic change of medulla in human thymic implant due to intravenous inoculation of primary HIV-1 isolate. J. Immunol. 160, 69–76.

Pantaleo, G., Graziosi, C., Demarest, J.F., Butini, L., Montroni, M., Fox, C.H., Orenstein, J.M., Kotler, D.P., Fauci, A.S., 1993. HIV infection is active and progressive in lymphoid tissue during the clinically latent stage of disease. Nature 362, 355–358.

Pantaleo, G., Menzo, S., Vaccarezza, M., Graziosi, C., Cohen, O.J., Demarest, J.F., Monte-fiori, D., Orenstein, J.M., Fox, C., Schrager, L.K., Margolick, J.B., Buchbinder, S., Giorgi, J.V., Fauci, A.S., 1995. Studies in subjects with long-term nonprogressive human immunodeficiency virus infection. New Engl. J. Med. 332, 209–216.

Prevot, S., Audouin, J., Andre-Bougaran, J., Griffais, R., Le Tourneau, A., Fournier, J.G., Diebold, J., 1992. Thymic pseudotumorous enlargement due to follicular hyperplasia in a human immunodeficiency virus seropositive patient, immunohistochemical and molecular biological study of viral infected cells. Am. J. Clin. Pathol. 97, 420–425.

Reimann, K.A., Li, J.T., Veazey, R., Halloran, M., Park, I., Karlsson, G.B., Sodroski, J., Letvin, N.L., 1996a. A chimeric simian/human immunodeficiency virus expressing a primary patient human immunodeficiency virus type 1 isolate env causes an AIDS-like disease after in vivo passage in rhesus monkeys. J. Virol. 70, 6922–6928.

Reimann, K.A., Li, J.T., Voss, G., Lekutis, C., Tenner-Racz, K., Racz, P., Lin, W., Montefiori, D.C., Lee-Parritz, D.E., Lu, Y., Collman, R.G., Sodroski, J., Letvin, N.L., 1996b. An env gene derived from a primary human immunodeficiency virus type 1 isolate confers high in vivo replication capacity to a chimeric simian/human immunodeficiency virus in rhesus monkeys. J. Virol. 70, 3198–3206.

Ringler, D.J., Wyand, M.S., Walsh, D.G., MacKey, J.J., Chalifoux, L.V., Popovic, M., Minassian, A.A., Sehgal, P.K., Daniel, M.D., Desrosiers, R.C., King, N.W., 1989. Cellular localization of simian immunodeficiency virus in lymphoid tissues. I. Immunohistochemistry and electron microscopy. Am. J. Pathol. 134, 373–383.

Sakuragi, S., Shibata, R., Mukai, R., Komatsu, T., Fukasawa, M., Sakai, H., Sakuragi, J., Kawamura, M., Ibuki, K., Hayami, M., Adachi, A., 1992. Infection of macaque monkeys with a chimeric human and simian immunodeficiency virus. J. Gen. Virol. 73, 2983–2987.

Shibata, R., Kawamura, M., Sakai, H., Hayami, M., Ishimoto, A., Adachi, A., 1991. Generation of a chimeric human and simian immunodeficiency virus infectious to monkey peripheral blood mononuclear cells. J. Virol. 65, 3514–3520.

Shimosato, Y., and Mukai, K. (1997). Tumors of the mediastinum. *In* "Atlas of Tumor Pathology," 3rd series, fascicle 21 vols. Armed Forces Institute of Pathology, Washington, DC.

Stoddart, C.A., Liegler, T.J., Mammano, F., Linquist-Stepps, V.D., Hayden, M.S., Deeks, S.G., Grant, R.M., Clavel, F., McCune, J.M., 2001. Impaired replication of protease inhibitor-resistant HIV-1 in human thymus. Nat. Med. 7 (6), 712–718.

Suster, S., Rosai, J., 1992. Thymus. In Sternberg, S.S. (Ed.), Histology for Pathologists. Raven Press, New York, pp. 261–277.

Toti, P., De Felice, C., Stumpo, M., Schurfeld, K., Di Leo, L., Vatti, R., Bianciardi, G., Buonocore, G., Seemayer, T.A., Luzi, P., 2000. Acute thymic involution in fetuses and neonates with chorioamnionitis. Hum. Pathol. 31 (9), 1121–1128.

Wallace, M., Waterman, P.M., Mitchen, J.L., Djavani, M., Brown, C., Trivedi, P., Horejsh, D., Dykhuizen, M., Kitabwalla, M., Pauza, C.D., 1999. Lymphocyte activation during acute simian/human immunodeficiency virus SHIV(89.6PD) infection in macaques. J. Virol. 73 (12), 10236–10244.

Weiss, R.A., Claphan, P.R., Weber, J.N., Dalgleish, A.G., Lasky, L.A., Berman, P.W., 1986. Variable and conserved neutralization antigens of human immunodeficiency virus. Nature 324, 572–575.

Wenig, B.M., Thompson, L.D.R., Frankel, S.S., Burke, A.P., Abbondanzo, S.L., Sester-henn, I., Heffner, D.K., 1996. Lymphoid changes of the nasopharyngeal and palatine tonsils that are indicative of human immunodeficiency virus infection: a clinicopathologic study of 12 cases. Am. J. Surgical Pathol. 20 (5), 572–587.

Wyand, M.S., Ringler, D.J., Naidu, Y.M., Mattmuller, M., Chalifoux, L.V., Sehgal, P.K., Daniel, M.D., Desrosiers, R.C., King, N.W., 1989. Cellular localization of simian immunodeficiency virus in lymphoid tissues. II. In situ hybridization. Am. J. Pathol. 134, 385–393.

Wykrzykowska, J., Rosenzweig, M., Veazey, R.S., Simon, M.A., Halvorsen, K., Desrosiers, R.C., Johnson, R.P., Lackner, A.A., 1998. Early regeneration of thymic progenitors in rhesus macaques infected with simian immunodeficiency virus. J. Exp. Med. 187, 1767–1778.